

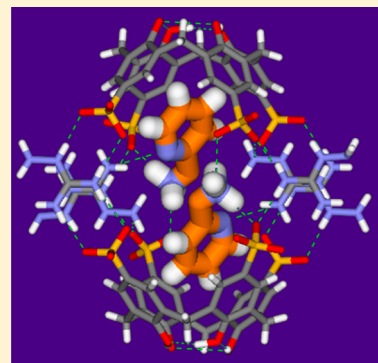
Crystallization-Driven Multicomponent Encapsulation of Coulombically Repulsive Guests

Mihail Barboiu,* Dan Dumitrescu,[†] Eddy Petit, Yves-Marie Legrand, and Arie van der Lee

Adaptive Supramolecular Nanosystems Group, Institut Européen des Membranes, ENSCM-UMII-CNRS UMR-5635, Place Eugène Bataillon, CC 047, F-34095 Montpellier, France

 Supporting Information

ABSTRACT: Coulombically repulsive cationic guests can be encapsulated in the multicomponent capsule hosts via favorable ion pairing, H-bonding intermolecular interactions. The inclusion of protonated and diprotonated 2-pycolyl amine guests in the calix[4]arene tetrasulfonate, tetrasodium salt C[4]) host is reminiscent with complex dynamic equilibria in solution. The addition of AG aminoguanidinium cations to such mixtures results in the formation of distinct crystalline bilayer and capsule architectures in the solid state. This shows that libraries of interexchanging supramolecular components may convert into robust solid state multicomponent capsules via constitutional crystallization.



The reversible noncovalent interactions between molecules serve to initiate specific self-assembly of supramolecular systems, toward the selection of complex functional architectures.^{1–3} Dynamic exchanges between different sets of molecular components of variable stoichiometry and conformations within variable exchanging supramolecular architectures may be usually observed in solution.^{4–10}

Multicomponent encapsulation might be considered as such a highly complex process. “Social multi-component isomers”, reported by Rebek et al.,⁴ shed light on interesting interactional kinetic and thermodynamic features on favorably interacting guests in a small space of a host-supermolecule, in solution. The deep cavitands reported by Gibb et al. behave as synergetic variable host–guest encapsulation in solution, caused by weak entropic effects.^{5–7} Fujita molecular flasks⁸ or molecular sponges^{9,10} allow the confined molecules to be complementarily fixed within the cavity of a host capsule in the solid state, thus practically limiting their molecular motions. The encapsulated guests follow a sort of “chemical collectivism”¹¹ rule, self-assembling themselves based on their own and capsule interactional behaviors.

Within this context, the covalent post-assembly modification^{12,13} or crystallization^{4–20} are some of the constitutional strategies used to control and to drive dynamic self-assembly toward kinetically stable functional systems, sorted out from a solution of exchanging components.²¹ If the interconverting components present similar solubility, it would be very difficult to sort out via crystallization. However, the lower solubility of one specific architecture might be induced by the addition of an external component, which may drive the system to form a crystalline network. Such a preorganized network in solution which cannot crystallize by itself, but that can form a crystalline

network in the solid state in the presence of target guest molecules, might be of interest as a complementary strategy to “molecular sponges” method.^{9,10}

Related to multicomponent encapsulation, an unexplored specific case is related to the “theoretically” unfavorable highly energetic coencapsulation of (multi)charged molecular components in the solid state, as a result of increased electrostatic repulsions concentrated within a confined small space. It may be a case of fundamental molecules like the neurotransmitters or other charged molecules under biological confinement.²²

We report here the case in which the cationic and dicationic guests may form inclusion complexes with anionic host molecules in solution which converts into unique compact packed species in the solid state via induced crystallization, by further addition of pro-crystallization external species. Remarkably, multicomponent encapsulation of Coulombically repulsive cationic guests results in the formation of well-defined capsule architectures in the solid state in a highly adaptive process. To this extent, herein we chose the calix[4]arene tetrasulfonate, tetrasodium salt C[4]), which is a well-known platform to generate a very wide range of interesting architectures: bilayers,^{23–28} mesoporous materials,^{29–32} capsules,^{33–35} and hybrids.^{36–38} Recent examples showed the formation of C[4] molecular capsules in the presence of guanidinium cations, G.^{39–43} In this study, aminoguanidinium, AG, was used instead of G, due to its ability to act as both H-bond donor and acceptor.⁴⁴ As model guest molecule we chose 2-pycolyl ammonium (PA) because it is sterically compatible with the calix[4]arene encapsulation and also because it can generate

Received: April 30, 2015

Published: June 8, 2015



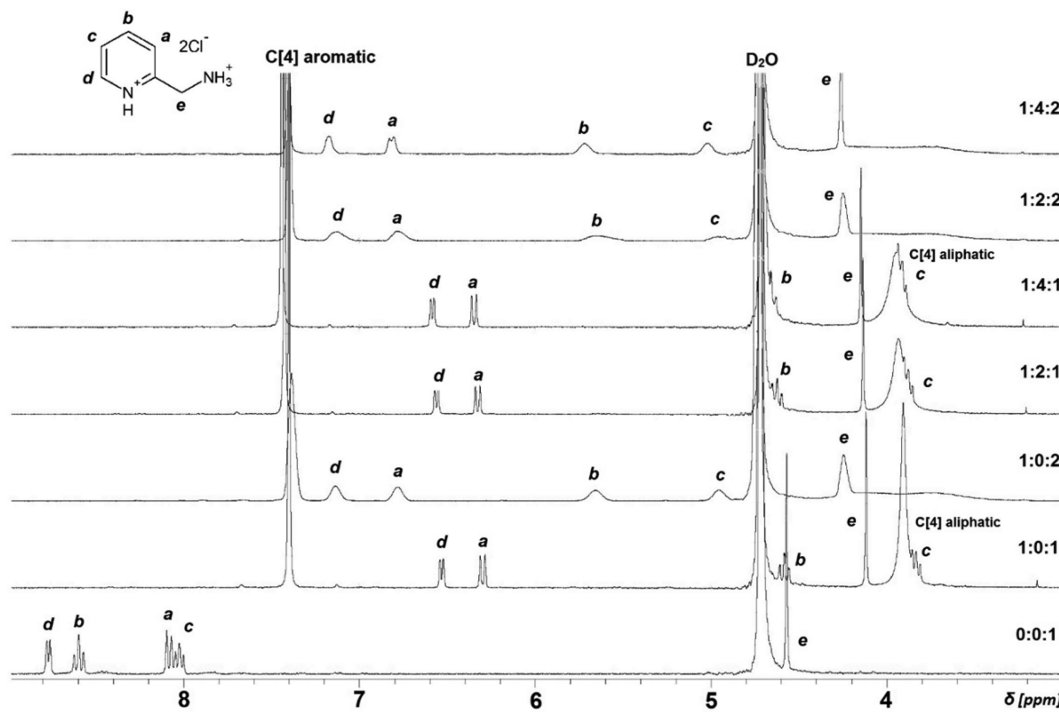


Figure 1. ^1H NMR spectra at different molar ratios of $\text{C}[4]:\text{AG:PAH}$ in D_2O at 25°C .

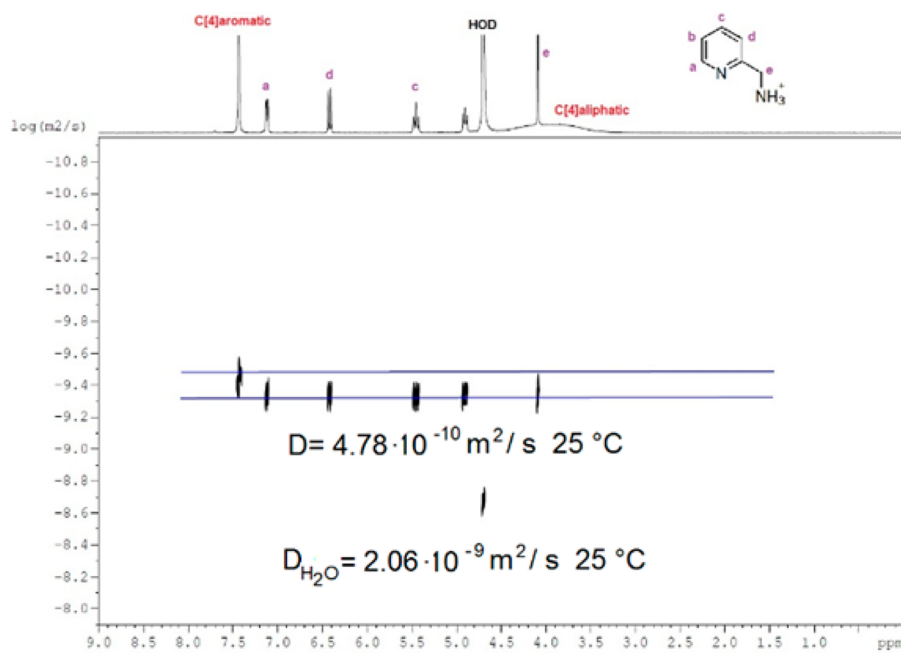


Figure 2. DOSY spectra of $\text{C}[4]_2\text{AG}_4\{\text{PAH}_2\}$.

mono- and dicationic species via protonation. In order to have a complete survey of collective multicomponent encapsulation of diverse cationic guests, a combinatorial screening of all possible combinations, was performed.

Calix[4]arenetetrasulfonate tetrasodium salt, **C[4]**, amino-guanidinium chloride, **AG**, and 2-pycolyl ammonium chloride, **PA**, or pycolyamine dihydrochloride, **PAH**, were mixed in water.

The proxy interactions between protonated pycolyl ammonium **PA** or **PAH** cations and **C[4]** anions can be detected in aqueous solution. The formation of the inclusion complexes is

confirmed by the strong upfield shifts of the protons of encapsulated **PAH** when compared with its spectra recorded in the absence of **C[4]** (Figure 1). The signals corresponding to the protons on the pyridinium are sharply reminiscent of low mobility of included molecule within the cavity. This results in a strong upfield shielding of the $\text{H}_\text{a}/\text{H}_\text{d}$ by about 1.5–2 ppm and a very strong shielding of the $\text{H}_\text{b}/\text{H}_\text{c}$ protons by about 4 ppm, respectively (Figure 1). The signals corresponding to the methylene groups in the **PAH** are shifted upfield by only about 0.2 ppm in the presence **C[4]**, probably being almost present at the entry of the **C[4]** cavity. This is consistent with a strong

inclusion of PAH by C[4], which is persistent in solution and on the NMR time scale. Moreover, this is reminiscent of a very fixed oriented encapsulation of PAH within the cavity of the C[4]: the PAH molecule has positioned the hydrophobic part of H_b/H_c protons in the deep part of the cavity, while the hydrophilically charged counterpart (H_a/H_d protons) is situated at the entrance of the cavity. The prevalent interactions observed are probably C–H–π between H_b/H_c protons of PAH and aromatic phenyls of C[4] and the ion-pairing between the sulfonate groups of C[4] and protonated charges moieties of PAH. The addition of a second equivalent of PAH results in a broadening and a decrease of the upfield of proton signals, showing that host–guest interactions are reminiscent of important dynamic exchanges between the encapsulated and solution-free molecules exchanging in and out of host molecules in solution (Figure 1). Very interestingly, the addition of aminoguanidinium cations, AG (in different molar ratios, Figure 1), do not induce any further changes in the encapsulation behaviors of PA or PAH cations by C[4] anions. The spectra are reminiscent of 1:1 PA or PAH:C[4] inclusion complexes which exchange their hosts in the excess of PA or PAH cations and are stable in the presence of additional AG cations that do not affect the equilibria in solution observed in their absence.

The DOSY spectra indicate the presence of the sole species in solution with a slightly larger diffusion coefficient for the resulting inclusion complex due to its bulkiness when compared with that of C[4] (Figure 2).

Slow evaporation of the aqueous solution of the C[4]:PA and C[4]:PAH (1:1 ratio) mixtures led to polycrystalline precipitates, which are mostly polymorphic and not suitable for accurate X-ray crystal structure determinations. Then, we observed that the addition of AG aminoguanidinium cations to such mixtures results in the formation of two pools of distinct yellow and red crystals and can be easily identified and selected (Figure 2). X-ray single crystal analysis showed that these crystals correspond to crystalline complexes of 2-pycolylamine hydrochloride (PA): the inclusion complex C[4]AG₂PA{PA}Na and the capsule-type C[4]₂AG₄{PA₂}Na₂, respectively.⁴⁵ When using bis-protonated 2-pycolyl-amine dihydrochloride (PAH) instead, only one type of crystal has been obtained, corresponding to a second, distinct capsule-type complex C[4]₂AG₄{PAH₂} (Figure 3).

The inclusion complex of monoprotonated PA, C[4]-AG₂{PA}PANa, is particularly interesting, as it contains two distinct internal PA_i and external PA_e molecules. The PA_i one is confined inside the C[4], while the PA_e acts as an external “lid” for the supramolecular complex. Both PA molecules are anchored via H-bonding of ammonium groups to sulfonate groups of C[4] and are interconnected via an intermolecular H-bond between the ammonium of the confined internal PA_i and the pyridine nitrogen of the external PA_e (Figure 4a). In the crystal, the hydrophobic–hydrophilic bilayer structure of C[4] is stabilized via H-bonded sheets of AG and PA_e cations and sulfonate moieties of C[4].⁴⁵ This induces an up–down arrangement of C[4] in the cone conformation that affords free space defined by internal pocket of C[4] component, available to PA_i guest molecules during the assembly of the crystal lattice (Figure 4b).

The second inclusion complex of PA, C[4]₂AG₄{PA₂}Na₂, consists of two C[4] molecules with their upper rims connected by four aminoguanidinium AG molecules (Figure 4c). This arrangement leads to a large internal cavity, which can

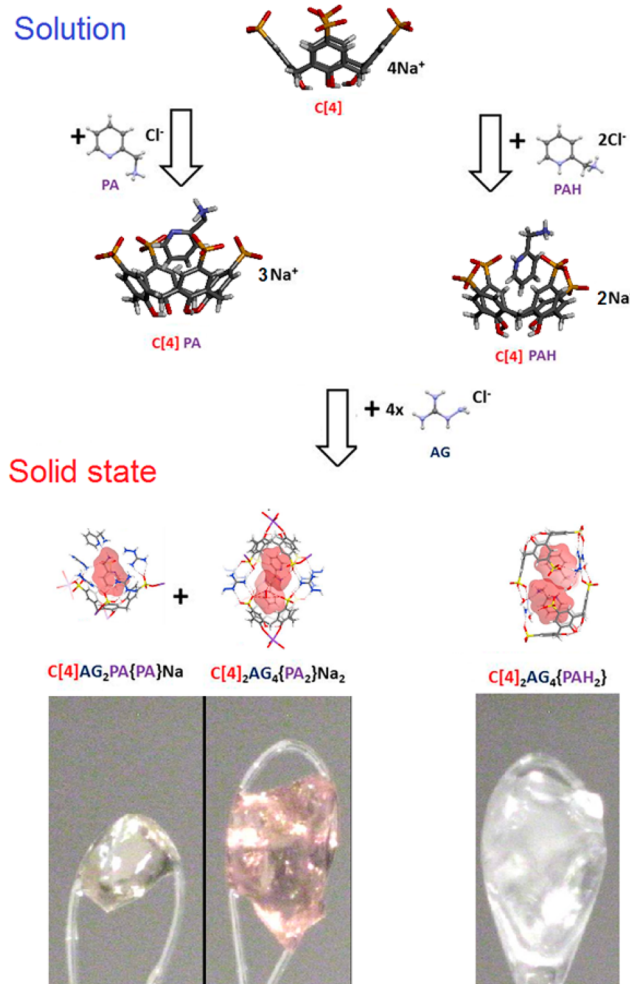


Figure 3. Synthetic strategy used to obtain the crystalline multi-component capsules. 2-Pycolyl ammonium, PA, is shown with its Connolly molecular surface when encapsulated, while calix[4]arene tetrasulfonate (C[4]), aminoguanidinium (AG), end-capping sodium cations, and water molecules are shown as capped sticks.

fit two Coulombically repulsive charged monoprotonated molecules PA (centroid–centroid distance of ~6.03 Å). Structural stability is increased by strong H-bonding of PA guests via donor H-bonding of ammonium groups to sulfonate groups and acceptor H-bonding of pyridine nitrogen to AG constituents. The compensation of the overall charge of the complex is satisfied by the presence of two Na⁺ ions, which connect adjacent capsule lower rims. In the crystal lattice the C[4]₂AG₄{PA₂}Na₂ capsules pack into parallel layers which are alternately stratified above each other. The C[4] components of the capsules are in van der Waals contact and form an alternate bilayer structure as previously observed (Figure 4d).

Very interestingly, when double protonated 2-pycolyl ammonium PAH is used as guest, only one single crystal structure is obtained, C[4]₂AG₄{PAH₂}, corresponding to the C[4]:PAH 2:2 inclusion complex (Figure 4e). In the complex C[4]AG₄{PAH₂} the previously observed positive charge compensation by the Na⁺ cations is no longer needed and thus it does not appear in the structure. Both PA molecules are anchored via H-bonding of ammonium groups to sulfonate groups of C[4] and present almost the same spatial disposition within the inner space of the capsule, despite the increase of the overall repulsive charges (centroid–centroid distance of about

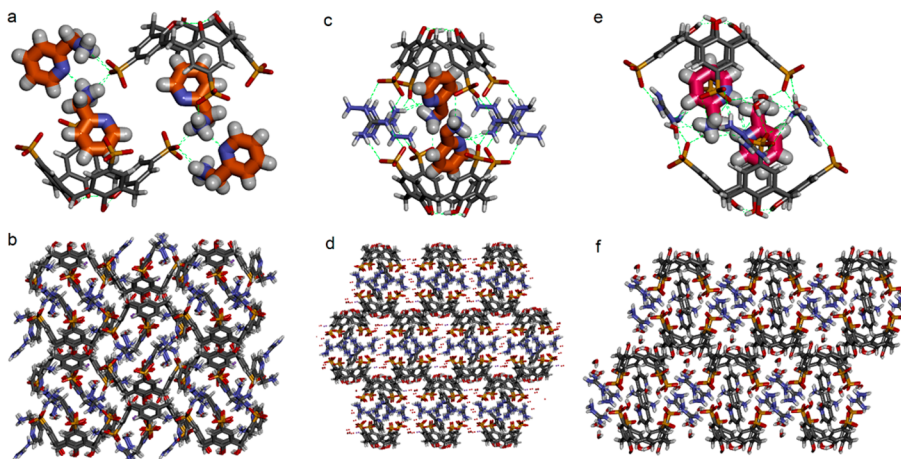


Figure 4. X-ray structures of the capsule-type systems. Side view and the crystal packing of the inclusion complexes: (a,b) $\text{C}[4]\text{AG}_2\text{PA}\{\text{PA}\}\text{Na}$, (c,d) $\text{C}[4]_2\text{AG}_4\{\text{PA}_2\}\text{Na}_2$, and (e,f) $\text{C}[4]_2\text{AG}_4\{\text{PAH}_2\}$.

6.61 Å). Several water molecules are incorporated into the capsule in order to complete the H-bond network. In contrast with the previous monoprotonated $\text{C}[4]_2\text{Ag}_4\{\text{PA}_2\}\text{Na}_2$, the donor H-bonding pyridinium $\text{PyN}^+ \cdots \text{H}$ group of double protonated PAH is H-bonded by a bridging water molecule, which is simultaneously H-bonded to two sulfonate groups in the network. In this case the capsule is more tightly packed, due to the increased charge of the dicationic guest. This tighter packing has interesting consequences on the arrangement and H-bonding of the AG. Compared to the monoprotonated PA inclusion structure, $\text{C}[4]_2\text{AG}_4\{\text{PA}_2\}\text{Na}_2$, where only the guanidinium part of AG takes part in H-bonded network, the AG molecules in the dicationic inclusion complex of PAH, $\text{C}[4]_2\text{AG}_4\{\text{PAH}_2\}$, are completely integrated into the network as via guanidinium moiety acting as hydrogen bond donors for the sulfonate groups and via amino moiety acting as hydrogen bond acceptors for the water molecules. In the crystal lattice the $\text{C}[4]_2\text{AG}_4\{\text{PAH}_2\}$ capsules also pack into parallel layers which are alternately stratified above each other. However, the layered structures of C[4] components are stabilized via H-bonded sheets of AG cations and sulfonate moieties of neighboring C[4] tethers (Figure 4f).

In order to better understand the source of this structural diversity we looked closely at the host–guest interactions between the pycolyl residue and the C[4] inner surface. In capsule $\text{C}[4]\text{AG}_2\{\text{PA}\}\text{PANa}$ the encapsulated pycolyl guest is stabilized inside the C[4] cavity by the C–H \cdots π interactions between the H4 and H5 protons of the pycolyl moiety and the phenyl rings of C[4], with contact lengths of 2.94 and 2.89 Å, respectively. In the second inclusion complex of PA, $\text{C}[4]_2\text{AG}_4\{\text{PA}_2\}\text{Na}_2$, the H3 and H5 protons of the pyridyl ring take part in CH \cdots π interactions with two opposing calix[4]arene rings of 2.82 and 2.78 Å, respectively. Finally, in the case of $\text{C}[4]_2\text{AG}_4\{\text{PAH}_2\}$ the calix[4]arene “wraps” around the guest, with the pyridinium ring sandwiched between two opposing phenyls with π–π-stacking contacts of 3.92 and 4.39 Å. The close host–guest proximity is also due to C–H \cdots π contacts with the H4, H5, and H6 of the pyridine ring and the calixarene interior (2.83, 2.68, and 2.87 Å). No significant π–π stacking interactions have been observed between the pycolyl guests and the calix[4]arene in all cases.

NCI plots^{46,47} were performed on all capsules for better understanding of the specific interactions occurring between the host and guest molecules. Although the host–guest

contacts vary in strength for each individual case, the C[4] molecule always seems to provide a pocket of weakly attractive van der Waals interactions for the pycolyl guests (Figure 5).

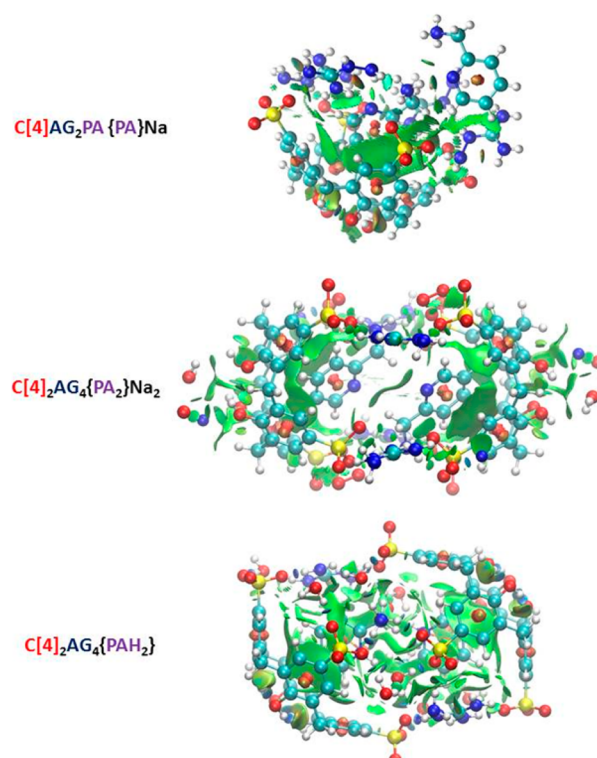


Figure 5. NCI plots of the structures obtained at 0.4 a.u. Green surfaces represent weak attractive interactions such as van der Waals forces, blue surfaces strong attractive interactions such as H-bonds, while red surfaces represent steric repulsions.

This would indicate that, although weak contacts dictate the supramolecular arrangement of the molecules, the main driving force in this case is the steric complementarity between the two species, i.e., filling the C[4] cavity, as well as strong charge interactions between oppositely charged moieties (ammonium and pyridinium moieties of the guests and sulfonate moieties of the host molecules).

Table 1. X-ray Diffraction Data Collection and Refinement

	C[4]AG ₂ PA{PA}Na	C[4] ₂ AG ₄ {PA ₂ }Na ₂	C[4]AG ₄ (PAH) ₂
Formula	C ₈₄ H ₁₀₂ N ₂₄ Na ₂ O ₃₃ S ₈	C ₃₆ H ₄₀ N ₁₀ NaO ₂₀ S ₄	C ₃₆ H ₅₆ N ₁₀ O ₂₂ S ₄
SG	P2 ₁ /n	P2 ₁ /n	P $\bar{1}$
<i>a</i> (Å)	16.6234(9)	11.7300(5)	12.5102(5)
<i>b</i> (Å)	14.1631(8)	30.0399(11)	13.4656(5)
<i>c</i> (Å)	20.9416(11)	14.0781(7)	15.4021(6)
α (deg)	90	90	65.072(4)
β (deg)	102.545(5)	95.903(4)	80.169(3)
γ (deg)	90	90	83.094(3)
<i>V</i> (Å ³)	4812.7(5)	4934.4(4)	2314.96(17)
<i>Z</i>	2	4	2
size (mm ³)	0.20 × 0.50 × 0.55	0.30 × 0.60 × 0.60	0.40 × 0.50 × 0.60
ρ (g cm ⁻³)	1.572	1.459	1.591
resolution (Å)	0.73	0.73	0.73
<i>N</i> _{reftot}	24273	24304	18628
<i>N</i> _{refls}	7545	9148	9143
<i>R</i> _{int}	0.100	0.030	0.029
$\langle \sigma(I)/I \rangle$	0.0886	0.0471	0.0498
<i>N</i> _{par}	685	667	685
<i>R</i> ₁	0.0820	0.1304	0.0544
<i>wR</i> ₂	0.0955	0.1347	0.0554
GOF	1.0444	1.0500	1.1075

Concluding Remarks. Collective encapsulation of Coulombically repulsive molecular cationic guests results in the generation of structural diversity of self-assembled multi-component host layers and capsules. The generation of host–guest complexes in solution results in the formation of equilibrating mixture of subcomponents that can only be identified as simply inclusion complexes of C[4]:PA and C[4]:PAH probably in equilibrium with more complex polymeric or capsule architectures. The addition of external AG aminoguanidinium cations to such mixtures results in the (co)formation of unique solid state bilayer and capsule species via crystallization.

These superstructures are a result of fine interplay between H-bonding and electrostatic interactions with weak hydrophobic van der Waals interactions which can synergistically dictate the nature of resulting inclusion complexes with different stoichiometries and geometries. Regardless, it appears that the main driving forces for encapsulation are the steric compatibility as well as the strong electrostatic interactions between the C[4] anionic host and cationic guests. By increasing the complementarity between the host and guest, and thus changing the balance between the electrostatic forces, only one type of complex can be obtained. The addition of AG aminoguanidinium cations is of crucial importance for capsule preformation in solution and is certainly responsible for their crystallization in the solid state.

The confined positively charged repulsive guests are synergistically fixed within the cavity of the cage, thus practically limiting their molecular motion under confined conditions. Within this context their structures and their interactive behaviors under confined conditions can be observed and elucidated. This refers directly to a variety of new phenomena that can be investigated and determined to become of crucial relevance for many chemical and biological scenarios.

EXPERIMENTAL SECTION

NMR Experiments. ¹H NMR experiments were performed on an ARX 300 MHz Bruker spectrometer in D₂O with the use of the residual solvent peak as reference. In the case of the NMR experiments 10 mg of the corresponding crystals obtained by the method described above were dissolved in 0.5 mL D₂O. 2D-DOSY (diffusion-ordered spectroscopy) NMR experiments were performed at 298 K with a Bruker Dual z-gradient probe head capable of producing gradients in the z direction with strength 55 G cm⁻¹. The DOSY spectra were acquired with the ledbpgr2s pulse program (2D sequence for diffusion measurement using echo and led with bipolar gradient pulse⁴⁸). All spectra were recorded with 8 K time domain data points in the F2 frequency axis and 32 experiments (F1). The gradient strength was logarithmically incremented in 32 steps from 2% up to 95% of the maximum gradient strength. All measurements were performed with a diffusion delay D of 80 ms in order to keep the relaxation contribution to the signal attenuation constant for all samples. The gradient pulse length d was 5 ms in order to ensure full signal attenuation. The diffusion dimension of the 2D DOSY spectra was processed by means of the Bruker Topspin software (v 2.1).

X-ray Single Crystal Diffraction Data Collection and Data Refinement (Table 1). Crystal evaluation and data collection were performed on an Agilent Gemini-S diffractometer with sealed-tube Mo K α radiation using the *CrysAlis Pro* program⁴⁹ (Agilent, 2012). The same program was used for the integration of the data using default parameters, the correction for Lorentz and polarization effects, and for the empirical absorption correction using spherical harmonics employing symmetry-equivalent and redundant data. In the presence of significant anomalous scattering and a chiral space group, Friedel pairs were not merged. The crystal structures were solved using the ab initio iterative charge flipping method with parameters described elsewhere⁵⁰ using the *Superflip* program,⁵¹ and they were refined using full-matrix least-squares procedures as implemented in *CRYSTALS*⁵² on all independent reflections with $I > 2s(I)$.

In the crystal structure of C[4]AG₂{PA₂}Na the water molecule bound to the sodium atom has an occupancy factor of 50%, which means that Na has 50% octahedral coordination by oxygen and 50% square pyramidal coordination.

The crystal structure of C[4]₂AG₄{PA₂}Na₂ has a high degree of disorder which can, however, not be modeled properly. The four nonbonded water molecules have site occupancy factors of 0.5. The hydrogen atoms of these water molecules could not be located from

difference Fourier maps and it was decided not to place geometrically them because of the complexity of the hydrogen-bond network. The *R*-factors of the refinement remain relatively high, because of the nonmodeled disorder, and in spite of the rather good quality indicators of the data set (R_{int} and $\langle \sigma(I)/I \rangle$).

The hydrogen atom positions of the water molecule in the crystal structure of C[4]AG₄(PAH)₂ were all located in difference Fourier maps and have been refined with distance and angle restraints and, for one of them also, with shift limiting restraints. Despite the logical hydrogen donor and acceptor scheme, some hydrogen atoms of neighboring water molecules have rather close intermolecular HH distances (around 1.9 Å).

The X-ray crystallographic coordinates for structures reported in this paper have been deposited at the Cambridge Crystallographic Data Centre, under deposition numbers CCDC 1017061–1017063. These data can be obtained free of charge from Cambridge Crystallographic Data Centre (http://www.ccdc.cam.ac.uk/data_request/cif).

■ ASSOCIATED CONTENT

Supporting Information

Crystallographic CIF files. The Supporting Information is available free of charge on the ACS Publications website at DOI: 10.1021/acs.cgd.5b00596.

■ AUTHOR INFORMATION

Corresponding Author

*E-mail: mihail-dumitru.barboiu@univ-montp2.fr.

Present Address

[†]C.D. Nenitzescu, Center for Organic Chemistry, Romanian Academy, Spl. Independentei 202b, Bucharest, Romania and SARA Pharm Solutions, 266–268 Calea Rahovei, 050912, Bucharest, Romania.

Author Contributions

The manuscript was written through contributions of all authors. All authors have given approval to the final version of the manuscript.

Funding

This work was conducted within the framework of DYNANO, PITN-GA-2011-289033 (www.dynano.eu) and ANR “LABEX Chemisyst” ANR-10-LABX-05-01 (D.D.) awarded by “Pole Balard” Montpellier.

Notes

The authors declare no competing financial interest.

■ DEDICATION

Dedicated to Prof. Jean-Marie Lehn on the occasion of 50th anniversary of his laboratory.

■ REFERENCES

- (1) Lehn, J.-M. *Chem. Soc. Rev.* **2007**, *36*, 151–160.
- (2) Thomas, J. A. *Chem. Soc. Rev.* **2007**, *36*, 856–868.
- (3) Northrop, B. H.; Yang, H.-B.; Stang, P. J. *Inorg. Chem.* **2008**, *47*, 11257–11268.
- (4) Ajami, D.; Theodorakopoulos, G.; Petsalakis, I. D.; Rebek, J., Jr *Chem.—Eur. J.* **2013**, *19*, 17092–17096.
- (5) Laughrey, Z.; Gibb, B. C. *Chem. Soc. Rev.* **2011**, *40*, 363–386.
- (6) Gan, H.; Gibb, B. C. *Chem. Commun.* **2013**, 1395–1397.
- (7) Gan, H.; Gibb, B. C. *Chem. Commun.* **2011**, *47*, 1656–1658.
- (8) Inokuma, Y.; Kawano, M.; Fujita, M. *Nat. Chem.* **2011**, *3*, 249–358.
- (9) Inokuma, Y.; Yoshioka, S.; Ariyoshi, J.; Arai, T.; Hitora, Y.; Takada, K.; Matsunaga, S.; Rissanen, K.; Fujita, M. *Nature* **2013**, *495*, 461–466.
- (10) Corrigendum. *Nature* **2013**, *501*, 262.
- (11) Menger, F. *Angew. Chem., Int. Ed.* **1991**, *30*, 1086–1089.
- (12) Arnal-Herault, C.; Michau, M.; Pasc-Banu, A.; Barboiu, M. *Angew. Chem., Int. Ed.* **2007**, *46*, 4268–4272.
- (13) Kaucher, M. S.; Harrell, W. A.; Davis, J. T. *J. Am. Chem. Soc.* **2006**, *128*, 38–39.
- (14) Angelin, M.; Vongvilai, P.; Fischer, A.; Ramström, O. *Chem. Commun.* **2008**, 768–770.
- (15) Angelin, M.; Vongvilai, P.; Fischer, A.; Ramström, O. *J. Org. Chem.* **2008**, *73*, 3593–3595.
- (16) Dumitru, F.; Petit, E.; van der Lee, A.; Barboiu, M. *Eur. J. Inorg. Chem.* **2005**, 4255–4262.
- (17) Legrand, Y.-M.; van der Lee, A.; Barboiu, M. *Inorg. Chem.* **2007**, *46*, 9083–9089.
- (18) Legrand, Y. M.; Dumitru, F.; van der Lee, A.; Barboiu, M. *Chem. Commun.* **2009**, 2667–2669.
- (19) Dumitru, F.; Legrand, Y.-M.; Petit, E.; van der Lee, A.; Barboiu, M. *Dalton Trans.* **2012**, *41*, 11860–11865.
- (20) Kocsis, I.; Dumitrescu, D.; Legrand, Y.-M.; van der Lee, A.; Grosu, I.; Barboiu, M. *Chem. Commun.* **2014**, *50*, 2621–2623.
- (21) Barboiu, M. *Top. Curr. Chem.* **2012**, *322*, 33–54.
- (22) Dougherty, D. A. *Science* **1996**, *271*, 163–168.
- (23) Drljaca, A.; Hardie, M. J.; Raston, C. L.; Spiccia, L. *Chem.—Eur. J.* **1999**, *5* (8), 2295–2299.
- (24) Selkti, M.; Coleman, A. W.; Nicolis, I.; Douteau-Guével, N.; Villain, F.; Tomas, A.; de Rango, C. *Chem. Commun.* **2000**, 161–162.
- (25) Da Silva, E.; Nouar, F.; Nierlich, M.; Rather, B.; Zaworotko, M. J.; Barbey, C.; Navaza, A.; Coleman, A. W. *Cryst. Eng.* **2003**, *6*, 123–135.
- (26) Lazar, A.; Da Silva, E.; Navaza, A.; Barbey, C.; Coleman, A. W. *Chem. Commun.* **2004**, 2162–2163.
- (27) Ling, I.; Alias, Y.; Sobolev, A. N.; Raston, C. L. *CrystEngComm* **2010**, *12*, 1869–1875.
- (28) Ling, I.; Sobolev, A. N.; Alias, Y.; Raston, C. L. *CrystEngComm* **2013**, *15*, 2888–2896.
- (29) Nichols, P. J.; Raston, C. L.; Steed, J. W. *Chem. Commun.* **2001**, 1062–1063.
- (30) Zheng, G.; Li, Y. Y.; Guo, H.-D.; Songa, S.-Y.; Zhang, H.-J. *Chem. Commun.* **2008**, 4918–4920.
- (31) Ling, I.; Alias, Y.; Sobolev, A. N.; Byrne, L. T.; Raston, C. L. *Chem.—Eur. J.* **2010**, *16*, 6973–6982.
- (32) Brancatelli, G.; De Zorzi, R.; Hickey, N.; Siega, P.; Zingone, G.; Geremia, S. *Cryst. Growth Des.* **2012**, *12*, 5111–5117.
- (33) Airey, S.; Drljaca, A.; Hardie, M. J.; Raston, C. L. *Chem. Commun.* **1999**, 1137–1138.
- (34) Leverd, P. C.; Berthault, P.; Lance, M.; Nierlich, M. *Eur. J. Org. Chem.* **2000**, 1332–1339.
- (35) Dalgarno, S. J.; Atwood, J. L.; Raston, C. L. *Cryst. Growth Des.* **2006**, *6* (1), 174–180.
- (36) Makha, M.; Raston, C. L.; Sobolev, A. N.; White, A. H. *Chem. Commun.* **2008**, 1066–1067.
- (37) Shkurenko, O.; Suwinska, K.; Coleman, A. W. *CrystEngComm* **2008**, *10*, 821–823.
- (38) Lin, R.-G.; Long, L.-S.; Huang, R.-B.; Zheng, L.-S. *Cryst. Growth Des.* **2008**, *8* (3), 791–794.
- (39) Ward, M. D. *Cryst. Growth Des.* **2013**, *13* (7), 3197–3200.
- (40) Legrand, Y. M.; van der Lee, A.; Barboiu, M. *Science* **2010**, *329*, 299–302.
- (41) Liu, Y.; Ward, M. D. *Cryst. Growth Des.* **2009**, *9*, 3859–3861.
- (42) Legrand, Y.-M.; Gilles, A.; Petit, E.; van der Lee, A.; Barboiu, M. *Chem.—Eur. J.* **2011**, *17*, 10021–10028.
- (43) Dumitrescu, D.; Legrand, Y.-M.; Petit, E.; van der Lee, A.; Barboiu, M. *Chem. Commun.* **2014**, *50*, 14086–14088.
- (44) Dumitrescu, D.; Legrand, Y.-M.; Dumitrescu, F.; Barboiu, M.; van der Lee, A. *Cryst. Growth Des.* **2012**, *12*, 4258–4263.
- (45) Atwood, J. L.; Barbour, L. J.; Hardie, M. J.; Raston, C. L. *Coord. Chem. Rev.* **2001**, *222*, 3–32.
- (46) Johnson, E. R.; Keinan, S.; Sanchez, P. M.; Contreras-Garcia, J.; Cohen, A. J.; Yang, W. W. *J. Am. Chem. Soc.* **2010**, *132*, 6498–6506.

- (47) Contreras-Garcia; Johnson, E. R.; Keinan, S.; Chaudret, R.; Piquemal, J. P.; Beratan, D. N.; Yang, W. *J. Chem. Theory Comput.* **2011**, *7*, 625–632.
- (48) Wu, D.; Chen, A.; Johnson, C. S., Jr. *J. Magn. Reson. A* **1995**, *115*, 260–264.
- (49) Agilent. *CrysAlis PRO*; Agilent Technologies, Yarnton, England, 2012.
- (50) van der Lee, A. *J. Appl. Crystallogr.* **2013**, *46*, 1306–1315.
- (51) Palatinus, L.; Chapuis, G. *J. Appl. Crystallogr.* **2007**, *40*, 786–790.
- (52) Betteridge, P. W.; Carruthers, J. R.; Cooper, R. I.; Prout, K.; Watkin, D. J. *J. Appl. Crystallogr.* **2003**, *36*, 1487.